Extracellular structure of polysialic acid explored by on cell solution NMR

Hugo F. Azurmendi*, Justine Vionnet*, Lauren Wrightson*, Loc B. Trinh†, Joseph Shiloach†, and Darón I. Freedberg*‡

*Laboratory of Bacterial Polysaccharides, Center for Biologics Evaluation and Research, Food and Drug Administration, 1401 Rockville Pike, Rockville, MD 20852-1448; and †Biotechnology Unit, MSC 5522, National Institute of Diabetes and Digestive and Kidney Diseases, National Institutes of Health, Bethesda, MD 20892

Communicated by John B. Robbins, National Institute of Child Health and Human Development, Bethesda, MD, May 10, 2007 (received for review December 17, 2006)

The capsular polysaccharide of the pathogens *Neisseria meningitidis* serogroup B and of *Escherichia coli* K1, α(2 → 8) polysialic acid (PSA), is unusual, because when injected into adult humans, it generates little or no antibody. In contrast, people infected with these pathogens generate specific serum antibodies. A structural study on cells is used to address this anomaly by characterizing antigen structures *in vivo*. We introduce on cell multidimensional solution NMR spectroscopy for direct observation of PSA on *E. coli* bacteria. Using ^{13}C,^{15}N-labeled PSA, we applied a combination of heteronuclear NMR methods, such as heteronuclear single quantum coherence, HNCA, and HNCO, *in vivo*. Analysis reveals that free and cell-bound PSA are structurally similar, indicating that the poor immunogenicity of PSA is not due to major structural differences between cells and purified PSA. The ^{13}C linewidths of PSA on cells are 2 to 3 times larger than the corresponding ones in free PSA. The possible implications of the differences between free and on cell PSA are discussed. In addition, we demonstrate the suitability of the method for *in vivo* kinetic studies.

carbohydrate structure | isotopically labeled carbohydrates | *in vivo* kinetics | triple resonance NMR

Polysaccharides are constituents of cell walls, define blood groups, and mediate cell–cell interactions and inflammatory and immune responses. Of interest is the presence of signature carbohydrates in cell walls of pathogenic bacteria, viruses, and cells affected by cancer, tuberculosis, or AIDS. In these cases, the specific polysaccharide could be targeted to produce vaccines. Indeed, polysaccharide and protein-polysaccharide conjugates from bacterial capsules are licensed vaccines (1).

The meningitis-causing bacteria, *Neisseria meningitidis* B and *Escherichia coli* K1, have polysialic acid (PSA) as their capsular polysaccharide (2). PSA is a linear homopolymer of α(2 → 8) Neu5Ac (*N*-acetyl neuraminic acid) (Fig. 1 blue) (3). PSA is atypical because it induces a weak or null immune response when administered to adults (4). Some attribute this effect to the presence of similar carbohydrates in humans (5–7). However, infection by these pathogens induces an age-dependent immune response to PSA (8–10), and antibodies elicited to *Neisseria meningitidis* B infection confer complete protection in mice (2). Interestingly, the same PSA is found on the surface of lung carcinoma and pituitary tumors (11). The finding that PSA-like antigens are expressed in healthy humans has restricted studies to animal models and, consequently, hampered the use of PSA as vaccine component (12–16). Efforts to obtain vaccines aimed at PSA but based on alternative components have been unsuccessful (17).

PSA can contain several differentiated motifs from those found in humans, such as lactones (Fig. 1, red) (18), specific helical forms (19, 20), or de-*N*-acetylated residues (21), which may constitute an opportunity for vaccine development. These motifs could provide an alternative explanation for the resulting poor immunogenicity of PSA if any of them would be found *in vivo* but not *in vitro*. In this study, we report a comparison between *in vivo* and *in vitro* PSA structures.

NMR can provide information on molecules in solution with atomic resolution at physiologically relevant pH and temperatures. In many cases, however, the cellular environment can influence molecular function or interactions, thereby limiting the utility of *in vitro* studies. For example, recent reports of *in cell* NMR studies showed that the cellular environment can play a role in protein folding (22). This is particularly important for polysaccharides, where isolation from the biologically relevant environment could affect antigen structure, and purification may induce chemical changes. Although polysaccharides have been studied in cells by high resolution-magic angle spinning NMR (23, 24), in this method, the cells are killed to prepare the densely packed sample required for high-speed rotation, which can modify antigen conformation. To investigate the *in vivo* structure of PSA, we used a genetically engineered *E. coli* strain that allowed selective isotopic enrichment of the capsular polysaccharide with ^{13}C and ^{15}N isotopes. Thus, setting precedent for powerful methodology that could be used to study a wide range of biological problems, we studied the polysaccharide in its natural environment by solution NMR techniques. Taking advantage of a low background signal, and using the sensitivity of NMR chemical shifts to probe structure, we looked for evidence of structural differences between *in vivo* and *in vitro* PSA, such as lactones or stable helices. Lactones are formed by condensation of the CO_2H group of one residue with OH-9 of the adjacent residue to yield a six-membered ring (Fig. 1) and have been reported to markedly reduce the antigenicity of PSA (18). The spiro arrangement rigidifies the polymer chain, generating a unique characteristic chemical shift pattern distinct from free PSA. Stable PSA helices should also show characteristic NMR spectra.

Results and Discussion

Genetically modified *E. coli* K12 strains EV36 (25) and EV239 (26) were used to obtain cells with ^{13}C and ^{15}N isotopically enriched PSA. EV36 is a K12 hybrid strain constructed to express a K1 capsule (i.e., PSA), and contains genes to catabolize, synthesize and polymerize Neu5Ac (*nanA*, *neuB*, and *neuS*, respectively). These genes are mutated in EV239 (27), preventing the consumption and production of Neu5Ac. This organism can import Neu5Ac thanks to the specific permease NanT (28); hence, with the introduction of the *neuS*-containing plasmid pWN609 (29) into EV239 cells (EV239^{+neuS}), addition of labeled Neu5Ac to the culture media produces cells with labeled PSA. Control experiments and ideal growing conditions for these cells

Author contributions: J.V. and D.I.F. designed research; H.F.A. performed research; H.F.A., L.W., L.B.T., and J.S. contributed new reagents/analytic tools; H.F.A. and D.I.F. analyzed data; and H.F.A. and D.I.F. wrote the paper.

The authors declare no conflict of interest.

Freely available online through the PNAS open access option.

Abbreviations: HSQC, heteronuclear single quantum coherence; PSA, polysialic acid; sw, spectral width.

‡To whom correspondence should be addressed. E-mail: daron.freedberg@fda.hhs.gov.

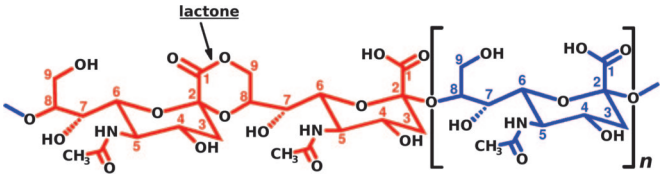

Fig. 1. Chemical structure of PSA (poly-α(2 → 8)Neu5Ac). The numbers identify carbon positions, and *n* can reach 200. Blue and red are used to differentiate the two possible forms the linkage can take. At neutral pH, most α(2 → 8) linkages are like the blue one, resulting in a highly flexible linear molecule. At low pH, the number of lactones increases, resulting in a rigidified structure.

expressing the capsule were determined by rocket immunoelectrophoresis (30) and NMR correlation experiments (data not shown).

A typical ^{1}H-^{13}C heteronuclear single quantum coherence (HSQC) NMR spectrum (31) performed on EV239^{+neuS} cells grown in the presence of ^{13}C,^{15}N-Neu5Ac is shown in Fig. 2*A*. The quality of the data is excellent, and spectra can be quickly acquired (≈20 min in this example). To assign the PSA signals *in vivo*, we measured ^{1}H-^{13}C HSQC spectra of ^{13}C,^{15}N free PSA and Neu5Ac, under similar conditions to on cell experiments. Fig. 2*B* shows overlays of those spectra with the respective reported assignments (32), revealing the clear differences in chemical shifts between monomer and polymer because of their distinct structures. Detailed comparison between free PSA (Fig. 2*B*, black spectrum) and EV239^{+neuS} spectra reveals that 10 of 27 peaks observed in the EV239^{+neuS} spectrum have essentially identical chemical shifts to free PSA. This result indicates not only that the cells have produced PSA, but also that PSA has the same structure on cells as in the free form. Further comparison with the β-Neu5Ac spectrum (Fig. 2*B*, red spectrum) confirmed the presence of unmetabolized Neu5Ac in cells, because the 10 β-Neu5Ac resonances are also observed in the EV239^{+neuS} spectrum. In addition, the two weak peaks observed at 62.6 ppm in the ^{13}C-dimension in cells are also observed in control experiments of Neu5Ac in LB (data not shown), but not with buffer (Fig. 2*B*). Their chemical shifts are very close to those reported for CH-9 resonances of Neu5Ac interacting with Ca^{2+} (33). This was confirmed by addition of $CaCl_2$ to the monomer in buffer (data not shown), strongly suggesting that the weak signals seen in cells are due to the residual Neu5Ac interacting with divalent cations. The remaining unmarked peaks, which are also observed in control experiments of EV239^{+neuS} cells grown in LB media with addition of unlabeled Neu5Ac, are background resonances due to media or cells.

Triple-resonance correlation experiments are important sources of information for assigning spectra of nitrogen containing molecules. However, the high molecular weight of cell-bound polysaccharide antigens could, in principle, abrogate signal because of short T_2 relaxation times. The relatively narrow ^{13}C lines in 1D spectra (15 to 30 Hz; data not shown) and good signal-to-noise ratio in 2D HSQCs suggested that triple-resonance experiments may work in this case. We used HNCO and HNCA correlation experiments (34, 35) to verify the *in vivo* chemical shift assignments of carbonyl, C5, and methyl. Initially, ^{1}H–^{15}N HSQC experiments were measured (data not shown) to determine the unreported ^{1}H and ^{15}N shifts of PSA as 7.97 and 124.3 ppm respectively, either free or *in vivo*, which were clearly different for the shifts measured for the residual Neu5Ac in cells of 7.90 and 124.5 ppm. Then, a 2D triple-resonance HNCO correlation experiment was acquired (Fig. 3*A*), from which the ^{13}CO chemical shift was determined, followed by a 2D HNCA (Fig. 3*B*) to obtain the $^{13}CH_3$ and ^{13}C5 chemical shifts. The resonances observed in these experiments for either PSA and

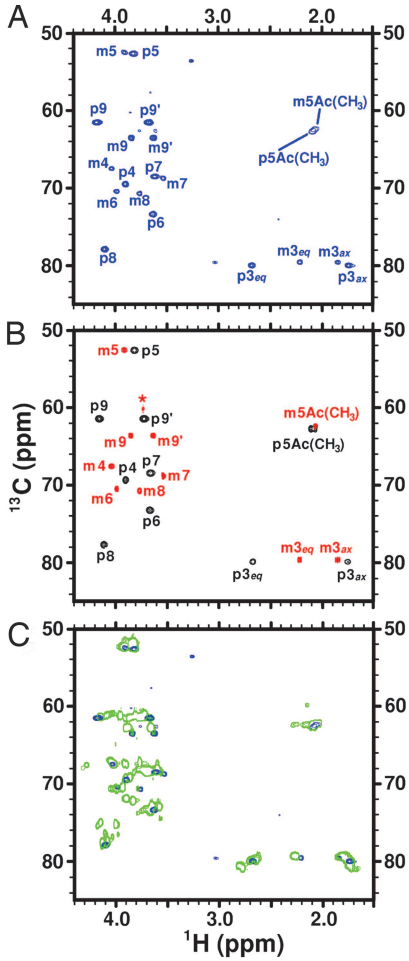

Fig. 2. ^{1}H^{-}^{13}C correlation spectra of PSA under several conditions. (*A* and *B*) Numbers identify carbons. *m*, monosaccharide; *p*, polysaccharide; *eq*, equatorial; *ax*, axial. (*A*) ^{1}H-^{13}C HSQC spectrum of EV239^{+neuS} cells grown in LB media containing ^{13}C,^{15}N-Neu5Ac. To improve resolution a spectral width of 40 ppm, with carrier frequency at 68 ppm, was used in the ^{13}C dimension, therefore the peaks between 1.50 and 3.10 ppm in the ^{1}H dimension are aliased in the ^{13}C dimension. These peaks have ^{13}C shifts that are 40 ppm lower than they appear. (*B*) The overlayed ^{1}H-^{13}C HSQC spectra of ^{13}C,^{15}N-Neu5Ac (red) and ^{13}C,^{15}N-PSA at neutral pH (black) clearly show the difference between the monomer (in the β-configuration) and polymer (α-configuration). *, identifies the Tris buffer signal. (*C*) ^{1}H-^{13}C HSQC spectrum of free ^{13}C,^{15}N-PSA at pH 4.0 (green), at which lactone formation is promoted, overlayed with spectrum (*A*). The number of green contours was purposely limited to better demonstrate the absence of lactones on cells.

Neu5Ac *in vivo* were identical to the observed *in vitro*. Attempts to obtain full chemical shift assignments for cell-bound PSA using long-range correlations from standard experiments such as HCCH-total correlation spectroscopy and heteronuclear multiple-bond correlation failed, probably because of shortened T_2s. Judging by the absence of changes in chemical shifts or appearances of new peaks, we conclude that the free and *in vivo* PSA structures are similar, with no direct evidence of other stable structural motifs.

To confirm the absence of inter-residue esterification in cell-bound PSA, a sample of free PSA at pH = 4.0 was kept at room temperature for 24 h to induce lactone formation (18). The resulting ^{1}H-^{13}C HSQC spectrum is displayed in green in Fig. 2*C* overlayed on the EV239^{+neuS} cells spectrum in blue. The spectrum clearly shows the appearance of several new peaks, distinct from the already identified signals, which are a result of lacton-

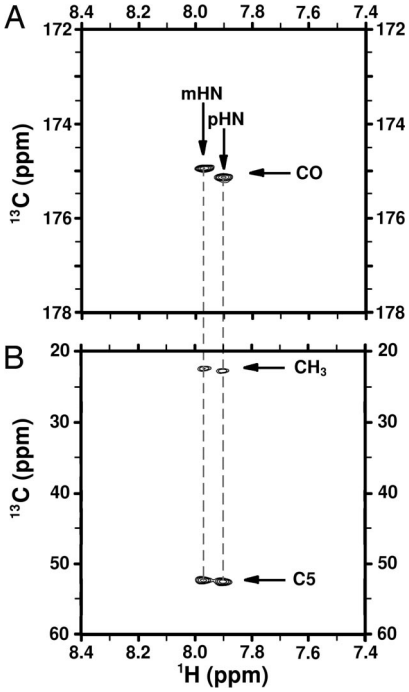

Fig. 3. Triple-resonance experiments correlating ^{1}H-^{15}N-^{13}C on EV239^{+neuS} cells grown with ^{13}C,^{15}N-Neu5Ac. The spectra show two sets of signals, which correspond to PSA (p) and Neu5Ac (m). (*A*) 2D-HNCO spectrum showing two signals correlating the amide ^{1}H with the ^{13}CO chemical shifts on the *N*-acetyl group through the ^{15}N atom. (*B*) 2D-HNCA spectrum correlating the amide ^{1}H chemical shift with $^{13}CH_3$ in the *N*-acetyl group and $^{13}C5$ through the ^{15}N atom.

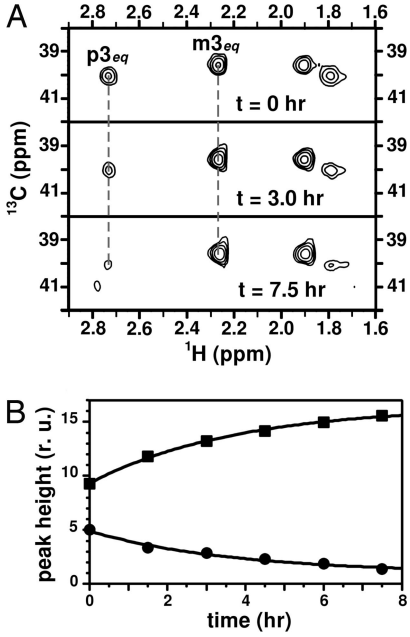

Fig. 4. Effects of exo-neuraminidase addition on NMR spectra, monitored through the peak height of the ^{13}CH-3 signals. (*A*) Region corresponding to ^{13}CH-3 signals from ^{1}H-^{13}C HSQC spectra of EV239^{+neuS} cells with ^{13}C,^{15}N-PSA before addition of the enzyme and at two representative times (indicated in the figure) after addition. The signals from PSA (labeled p) decrease in intensity as the monomer (m) increases. (*B*) Plot of the signal intensities from $m3_{eq}$ (■) and $p3_{eq}$ (●) as function of time after enzyme addition. Data fitting to single exponential functions (solid line) yielded identical rate constants ($0.27 \pm 0.01\ h^{-1}$) with opposite sign.

ization. After careful examination of the EV239^{+neuS} ^{1}H-^{13}C HSQC spectrum (down to the noise level) in search of possible resonances indicating lactone formation, we conclude that no evidence is available for such structures from the HSQC data. Because the presence of lactones at even $<10\%$ could have an important effect in antibody recognition, we further investigated the subject by *in vivo* and *in vitro* 1D ^{13}C NMR of PSA (data not shown). Detailed inspection of the regions expected to show signals due to lactone formation (especially near 167 ppm, where the resonance of the esterified C1 should appear) led us to conclude that under our experimental conditions, at least 96% of *in vivo* PSA is lactone free. Lastly, control experiments were performed to eliminate the possibility that the PSA precursor, CMP-Neu5Ac (36), had been detected in the HSQC spectra (data not shown). The CMP-Neu5Ac resonances could be clearly differentiated from those arising either from Neu5Ac or PSA. Therefore, none of the signals in the EV239^{+neuS} experiments was due to CMP-Neu5Ac.

Efforts to find ideal conditions in which all of the Neu5Ac is completely converted into PSA were unsuccessful, as evidenced by the presence of Neu5Ac signals in HSQCs. Interestingly, no Neu5Ac remains in the supernatant after centrifugation; thus, all Neu5Ac is cell-associated. Reduction of the amount of Neu5Ac added and delays on the time of addition only affected the total signal to noise ratio on the spectrum, but not the PSA to Neu5Ac signal ratio. Because it is known that the parent strain, EV36, uses Neu5Ac as an energy and carbon source (25), whereas in EV239 the gene expressing the Neu5Ac degrading enzyme, *nanA*, has been mutated, we reason that the intake of Neu5Ac, for the EV239 strain, is more efficient than its consumption.

Another concern relates to whether the cells are producing extracellular PSA. We know that PSA is associated with the cells because very little remains in the supernatant after centrifugation. To verify that PSA is located on the cell surface a Neu5Ac-cleaving enzyme, exo-neuraminidase, was added to the sample in the NMR tube. Because the enzyme has no access to the intracellular space, enzymatic hydrolysis of PSA would confirm the location of PSA on the cell's exterior. Polysaccharide cleavage was conveniently monitored by ^{1}H-^{13}C HSQC experiments, measuring the CH-3 peak heights from both PSA and Neu5Ac at various time intervals (Fig. 4*A*). As expected, the enzyme digests the PSA, as evidenced by the increasing peak height of the monosaccharide signal with time, in correlation with a decrease in signal intensity from PSA (Fig. 4*B*). In both cases, rate constants obtained from curve fittings to single exponential functions were indistinguishable, demonstrating *in vivo* kinetics as yet another application of on cell solution NMR.

Early in 1972, it was found that purified PSA did not elicit antibodies to *N. meningitidis* B and *E. coli* K1 (4). In 1981, it was reported that carbohydrates chemically resembling PSA are expressed during fetal development in humans (17). This observation suggested a rationalization to the poor response to PSA as the immune system being tolerant (17). Second, it raised the concern that a successful PSA-based vaccine could generate autoimmune reactions, limiting further studies of PSA-conjugate vaccines to animals (12, 14). However, no evidence has been presented in support of any of these hypotheses. Furthermore, the justified concern for an autoimmune response to PSA vaccines is inconsistent with the presence of PSA antibodies found in most healthy people without episodes of autoimmune diseases (14, 37). The effectiveness and safety of these vaccines in humans remain to be established.

Several questions should be answered to have a clear understanding of the above observations. One refers to possible structural differences between purified PSA and PSA *in vivo*. In the present work, we used NMR to examine PSA as present in living bacteria and compare it to purified PSA. Chemical shift

data from *in vivo* PSA at neutral pH, rule out the occurrence of significant amounts of lactones. Yet, lactone formation on cells could still be possible at lower pHs (such as in the urinary tract), or in hydrophobic environments. The overall conclusion from the present experiments at pH 7.0 is that PSA *on bacteria* is structurally similar, and likely identical, to free PSA. The environment can play an important role in dictating structural and dynamic properties of biomolecules, examples of which have been reported for proteins (22). Situations like mechanical stress (38), steric crowding, changes in pH, temperature, or hydrophobic environments, could have chemical or structural consequences providing defense mechanisms for the bacteria. This would be consistent with previous observations that antibodies to the capsular polysaccharide of *N. meningitidis* group B or *E. coli* K1 bind to the brains of infant rats *in vitro* but not *in vivo* (39). Schneerson and coworkers (16) suggest that the lack of tertiary structure in PSA combined with low energy binding at 37°C is the major cause of its poor immunogenicity. Another hypothesis is that fleeting conformations, like helices (40), could be stabilized under different conditions. In cases where the rate constant for conformational exchange is fast, NMR spectroscopy cannot always be used to distinguish between the conformers and instead yields spectra with averaged chemical shifts. In favorable cases, however, relaxation times or linewidths can be used as indicators of the underlying dynamics. A qualitative T_2 evaluation, comparing the peak linewidths in ^{13}C 1D spectra of PSA free and on cells, reveals that the linewidth of PSA on cells is approximately twice that of free PSA for all carbons, except those on the *N*-acetyl group and C5, for which the linewidths are ≈3 times larger. These differential relaxation times might reflect only the difference in environment for PSA and the restricted mobility of the end attached to the cell wall. On the other hand, they could also be an indication of subtle, yet important structural or dynamic differences that must be addressed. The method presented here seems promising to explore these possibilities, as well as studying the structural and dynamic characteristics of PSA-antibody interactions.

Materials and Methods

Preparation of ^{13}C,^{15}N-labeled Neu5Ac. The labeled monosaccharide was obtained by controlled hydrolysis of ^{13}C,^{15}N-labeled PSA (41) and purified by using a Mono Q column in an HPLC system (42). Labeled PSA was prepared by growing EV36 cells in minimum media supplemented with uniformly enriched ^{13}C-glucose and ^{15}N-NH_4Cl (Cambridge Isotope Laboratories, Andover, MA). Cells were grown by using a Bench top 14-liter Fermentor (New Brunswick Scientific, Edison, NJ) charged with 9 liters of basal salts media prepared as follows: (per liter) 6g Na_2HPO_4/3 g KH_2PO_4/0.5 g NaCl were dissolved in water and sterilized for 30 min at 121°C. The medium was allowed to cool to 37°C before 0.5 liter of a combined filtered-sterile solution was added: (per liter) 3 g ^{13}C-glucose/5 g ^{15}N-NH_4Cl/1.7 g yeast nitrogen base (without casamino acids and ammonium sulfate; BD Scientific, Sparks, MD), 10 mg streptomycin, and 0.001 g $CaCl_2$. The fermentor was then inoculated with 5% overnight inoculum and the culture was grown for 18 h at 37°C, with pH controlled at 7.0, using 5N NaOH solution. Dissolved oxygen was maintained at 30% air saturation by an adaptive control algorithm interfaced to an MD-Biostat system (Sartorius BBI System, Allentown, PA), by adjusting the agitation rate and the supply of air or oxygen (43). Off-line glucose measurements were done by using Yellow Spring Instruments (Yellow Spring, OH) biochemistry analyzer. A starter culture was grown from frozen stock of EV36 cells in LB media for 4 h, before transferring into the above-defined media and grown overnight with shaking at 250 rpm and 37°C. After 18 h fermentation, the 10-liter culture was diluted 1:1 with 0.2% hexadecyl trimethylammonium bromide (cetavlon) and allowed to precipitate at 4°C overnight with gentle mixing. The cetavlon pellet was collected by using a continuous centrifuge model T1P (Alfa Laval, Warminster, PA) and PSA-purified following the protocol by Vann and Freese (44).

Growing of EV239^{+neuS} Cells with ^{13}C,^{15}N-Neu5Ac and Sample Preparation. The plasmid pWN609 (29) contains the *neuS* gene to polymerize Neu5Ac. EV239 cells (27) containing pWN609 were grown from frozen stock in 20 ml of LB media for ≈16 h at 37°C with shaking at 180 rpm. EV239^{+neuS} cells grown without addition of Neu5Ac show negligible production of PSA. The capsule is produced by adding ≈1 mg of Neu5Ac (either labeled or unlabeled) to the culture media. Capsule production was monitored by rocket immunoelectrophoresis (45) and ^1H-^{13}C HSQC measurements. The procedure yields ≈200 mg of bacteria, which were collected by centrifugation (25 min at 2,000 × *g*) and gently resuspended in 250 μl of either LB or 20 mM buffer phosphate at pH 7.0, plus 50 μl of D_2O. The sample is transferred into Shigemi NMR tubes (Shigemi, Allison Park, PA) with the aid of long neck glass pipets (Wilmad, Buena, NJ).

NMR. NMR experiments were carried out at 37°C on a Bruker (Billerica, MA) Avance 700. For all multidimensional NMR experiments the ^1H carrier was placed on the HOD peak with a ^1H spectral width (sw) of 10 ppm, and recycle delay of 1 s. For PSA, either free or cell-bound, 1,024 complex points in the ^1H dimension and 256 on the ^{13}C dimension were measured. For Neu5Ac control experiments, 4,096 complex points were measured in the ^1H dimension. Additional relevant experimental parameters were: for ^1H-^{13}C HSQC the Bruker pulse program (Bpp) hsqcgpph was used with ^{13}C carrier at 68 ppm (sw 40 ppm); ^1H-^{15}N HSQC was measured under identical conditions, except that the ^{15}N carrier was set at 120 ppm; the HNCO was acquired by using the Bpp hncogp3d, only the ^1H-^{13}C plane was measured with ^{13}C carrier at 176 ppm (sw 10 ppm); for the HNCA, the Bpp hncagp3d was used with the same ^{15}N carrier as for the HNCO, and ^{13}C carrier at 38 ppm (sw 50 ppm). For both triple-resonance experiments, the magnetization transfer delays used were $1/4J_{HN} = 2.3$ ms and $1/4J_{NC'} = 12$ ms. The ^{13}C 1D experiments were measured at 176.05 MHz with ^{13}C carrier at 90 ppm (sw 200 ppm), acquiring 16,384 complex points (acquisition time 0.233 s) and a recycling delay of 1.5 s.

We thank Eric Vimr for providing bacterial strains EV36 and EV 239, W. F. Vann for providing the plasmid pWN609 and for useful discussions, M. S. Blake and D. A. Torchia for helpful discussions and support, R. Schneerson and E. Andereishcheva for help with techniques used in this paper, S. Norris for help with NMR instrumentation, and Y. Hi for providing HPLC time.

1. Robbins JB, Schneerson R, Anderson P, Smith DH (1996) *J Am Med Assoc* 276:1181–1186.
2. Robbins JB, McCracken GH, Gotschlich EC, Ørskov F, Ørskov I, Hanson LA (1974) *N Engl J Med* 290:12216–12220.
3. Bhattacharjee AK, Jennings HJ, Kenny CP, Martin A, Smith IC (1975) *J Biol Chem* 250:1926–1932.
4. Wyle FA, Artenstein MS, Brandt BL, Tramont EC, Kasper DL, Altieri PL, Berman SL, Lowenthal JP (1972) *J Infect Dis* 126:514–522.
5. Finne J, Leinonen M, Mäkelä, P. H (1983) *The Lancet* 2:355–357.
6. Griffiss JM, Yamasaki R, Estabrook M, Kim JJ (1991) *Trans R Soc Trop Med Hyg* 85(Suppl 1):32–36.
7. Troy FA (1992) *Glycobiology* 2:5–23.
8. Mäkelä H (1991) *Trans R Soc Trop Med Hyg* 85(Suppl 1):19–22.
9. Granoff DM, Kelsey SK, Bijlmer HA, Van Alphen L, Dankert J, Mandrell RE, Azmi FH, Scholten RJPM (1995) *Clin Diag Lab Immunol* 2: 574–582.
10. Jordens JZ, Williams JN, Jones GR, Christodoulides M, Heckels JE (2004) *Infect Immun* 72:6503–6510.

11. Samuel J, Bertozzi CR (2004) *Trends in Glycosience and Glycotechnology* 16:305–318.
12. Devi SJN, Robbins JB, Schneerson R (1991) *Proc Natl Acad Sci USA* 88:7175–7179.
13. Devi SJ, Zollinger WD, Snoy PJ, Tai JY, Constantini P, Norelli F, Rappuoli R, Frasch CE (1997) *Infect Immun* 65:1042–1052.
14. Zollinger W, Moran EE, Devi SJN, Frasch CE (1997) *Infect Immun* 65:1053–1060.
15. Toropainen M, Saarinen L, Wedege E, Bolstad K, Michaelsen TE, Aase A, Käythy H (2005) *Infect Immun* 73:4694–4703.
16. Stein DM, Robbins JB, Miller MA, Lin FYC, Schneerson R (2006) *Vaccine* 24:221–228.
17. Bruge J, Bouveret-Le Cam N, Danve B, Rougon G, Schulz D (2004) *Vaccine* 22:1087–1096.
18. Lifely MR, Gilbert AS, Moreno C (1981) *Carbohydr Res* 94:193–203.
19. Michon F, Brisson J-R, Jennings HJ (1987) *Biochem* 26:8399–8405.
20. Evans SV, Sigurskjold BW, Jennings HJ, Brisson J-R, To R, Tse WC, Altman E, Frosch M, Weisgerber C, Kratzin HD, *et al.* (1995) *Biochem* 34:6737–6744.
21. Moe GR, Dave A, Granoff DM (2006) *Mol Immunol* 43:1424–1431.
22. Dedmon MM, Patel CN, Young GB, Pielak GJ (2002) *Proc Natl Acad Sci USA* 99:12681–12684.
23. Szymanski CM, St Michael F, Jarrell HC, Li J, Gilbert M, Larocque S, Vinogradov E, Brisson JR (2003) *J Biol Chem* 278:24509–24520.
24. Gudlavalleti SK, Szymanski CM, Jarrell HC, Stephens DS (2006) *Carbohydr Res* 341:557–562.
25. Vimr ER, Aaronson W, Silver RP (1989) *J Bacteriol* 171:24509–24520.
26. Steenbergen SM, Wrona TJ, Vimr ER (1992) *J Bacteriol* 174:1099–1108.
27. Vimr ER (1992) *J Bacteriol* 174:6191–6197.
28. Ringerberg M, Lichtensteiger C, Vimr ER (2001) *Glycobiology* 11:533–539.
29. Andreishcheva EN, Vann WF (2006) *J Bacteriol* 188:1786–1797.
30. Vimr ER, McCoy RD, Vollger HF, Wilkison NC, Troy FA (1984) *Proc Natl Acad Sci USA* 81:1971–1975.
31. Schluecher J, Schwedinger M, Sattler M, Schmidt P, Schedletzky O, Glaser SJ, Sørensen OW, Griesinger C (1994) *J Biomol NMR* 4:301–306.
32. Vliegenthart JFG, Dorland L, van Halbeek H, Haverkamp J (1982) in *Sialic Acids: Chemistry, Metabolism and Function*, ed Schauer R (Springer-Verlag, New York), pp 127–172.
33. Jaques LW, Brown EB, Barrett JM, Brey WS, Jr, Weltner W, Jr (1977) *J Biol Chem* 252:4533–4538.
34. Kay LE, Ikura M, Tschudin R, Bax A (1990) *J Magn Reson* 89:496–514.
35. Grzesiek S, Bax A (1992) *J Magn Reson* 96:432–440.
36. Troy FA, Vijay IK, McCloskey MA, Rohr TE (1982) *Methods Enzymol* 83:540–548.
37. Kabat EA, Nickerson KG, Liao J, Grossbard L, Osserman EF, Glickman E, Chess L, Robbins JB, Schneerson R, Yang Y (1986) *J Exp Med* 164:642–654.
38. Marszalek PE, Oberhauser AF, Pang YP, Fernandez JM (1998) *Nature* 396:661–664.
39. Saukkonen K, Haltia M, Frosch M, Bitter-Süerman D, Leinonen M (1986) *Microbial Pathogenesis* 1:101–105.
40. Henderson TJ, Venable RM, Egan W (2003) *J Am Chem Soc* 125:2930–2939.
41. Cheng MC, Wang KT, Inoue S, Inoue Y, Khoo KH, Wu SH (1999) *Anal Biochem* 267:287–293.
42. Cheng MC, Lin CH, Lin HJ, Yu YP, Wu SH (2004) *Glycobiology* 14:147–155.
43. Hsiao J, Ahluwalia M, Kaufman JB, Clem TR, Shiloach J (1992) Ann N Y Acad Sci 665:320–333.
44. Vann WF, Freese S (1994) *Methods Enzymol* 235:304–311.
45. Vimr ER, McCoy RD, Vollger HF, Wilkison NC, Troy FA (1984) *Proc Natl Acad Sci USA* 81:1971–1975.